

Self-resonance after inflation: The case of α -attractor models

Daniel del-Corral^{1,2*}

^{1*}Departamento de Física, Universidade da Beira Interior, Rua Marquês D'Ávila e Bolama 6200-001 Covilhã, Portugal.

²Centro de Matemática e Aplicações da Universidade da Beira Interior, Rua Marquês D'Ávila e Bolama 6200-001 Covilhã, Portugal.

Corresponding author(s). E-mail(s): corral.martinez@ubi.pt;

Abstract

This work aims to explain the amplification of curvature perturbations on small scales arising from the phenomenon of self-resonance. By making a series expansion of the inflationary potential and employing perturbative techniques to solve for the inflaton field, we reformulate the Mukhanov-Sasaki equation into a Hill equation. Then, we derive expressions for the Floquet exponents corresponding to a potential having both cubic and quartic terms in its expansion. Our analytical results are then compared with numerical computations. Moreover, we propose potential applications including the generation of Primordial Black Holes, Scalar-Induced Gravitational Waves, and Oscillons.

1 Introduction

The cosmological models known as α -attractors [1–4] show an excellent agreement with Planck data [5] and have universal predictions of observables. For this reason, they have gained a lot of attention, as well as from the point of view of supergravity, where they are most naturally formulated. These models are characterized by the positive, real, dimensionless parameter α . In this work we study the post-inflationary phase of preheating [6] for this class of models, characterized by the inflaton's oscillation around its minimum. Specifically, our focus lies on the study of the amplification of curvature perturbations at small scales, driven by the phenomenon of self-resonance [7, 8], which arises when the potential deviates from quadratic behavior. While other works consider scenarios involving the coupling of the inflaton field to a daughter field,

a gauge field, or a fermionic field, in this work we consider these couplings to be small, directing our attention towards the self-interactions of the field, where the inflaton drives its fluctuations. Self-resonance is mainly based on the Taylor series expansion of the potential and posterior transformation of the perturbation equation into a Hill equation, which gives us the Floquet’s exponents governing the amplification of the perturbations. Usually, the potential during this period is approximated by a parabola [6, 9–11], since the terms in the expansion of the potential higher than quadratic are not relevant. However, as $\alpha < 1$, these terms become relevant, and thus self-resonance comes into play. The results obtained here can be extrapolated to any potential whose Taylor expansion is given by a quadratic part + higher order terms. Furthermore, the implications of our study extend to various phenomena. If the amplification from self-resonance reaches significant levels, perturbations could collapse and form Primordial Black Holes (PBHs) [12–15], Scalar-Induced Gravitational Waves (SIGWs) [16–20], or coherent structures known as oscillons [21–25], we leave this as a future project [26, 27]. The contents of this work are organized as follows. We begin in Sec. 2 by revisiting the α -attractor models. In Sec. 3 we study the effect of the self-resonance for a generic potential and compute the Floquet’s exponents. Then in Sec. 4 we show specifically for a T- and E-model the amplification of curvature perturbations and compare the results with a numerical computation. Sec. 5 focus on the importance of considering higher order terms in the expansion of the potential by comparing with the parabola approximation and finally in Sec. 6 we give some applications where this work can be useful. Conclusions are given in Sec. 7.

2 α -attractor models

There are two types of α -attractors, the so-called T- and E-models, whose potentials are given, respectively, by [4]

$$V_T(\phi) = 3\alpha M^2 \tanh^2 \left(\frac{\phi}{\sqrt{6\alpha}} \right), \quad (1a)$$

$$V_E(\phi) = \frac{3\alpha M^2}{4} \left(1 - e^{-\sqrt{\frac{2}{3\alpha}}\phi} \right)^2. \quad (1b)$$

Here, M is the inflaton mass, to be fixed by CMB normalization, ϕ is the scalar field and α is the parameter characterizing the models, with some constraints¹. Expanding the potentials around $\phi = 0$ we get

$$V_T(\phi) = \frac{M^2}{2}\phi^2 + \frac{\lambda_T}{4}\phi^4 + \dots, \quad (2a)$$

$$V_E(\phi) = \frac{M^2}{2}\phi^2 + \frac{\lambda_3}{3}\phi^3 + \frac{\lambda_E}{4}\phi^4 + \dots, \quad (2b)$$

¹In [28] it is given a lower bound for the parameter α , $\log_{10} \alpha = -4.2^{+5.4}_{-8.6}$ (95% C.L.), based on CMB constraints. We consider values of α above this lower bound for this work.

where the coefficients of the cubic and quartic terms, responsible for the anharmonic behavior of the field, are given in terms of the parameter α by

$$\lambda_T = -\frac{2M^2}{9\alpha}, \quad \lambda_3 = -M^2 \left(\frac{3}{2\alpha} \right)^{1/2}, \quad \lambda_E = \frac{7M^2}{9\alpha}. \quad (3)$$

This indicates that decreasing the parameter α enhances the importance of the cubic and quartic terms, even for relatively small values of ϕ .

3 Self-resonance for a generic potential

To obtain a general result for both T- and E-models, we will study self-resonance in potentials of the form

$$V(\phi) = \frac{M^2}{2}\phi^2 + \frac{\lambda_3}{3}\phi^3 + \frac{\lambda}{4}\phi^4. \quad (4)$$

The analysis is general and valid for every potential that can be written in this form, regardless of the presence of higher-order terms such as $\sim \phi^5$, $\sim \phi^6$, \dots

3.1 Perturbation theory for anharmonic oscillators

The background dynamics of the inflaton field ϕ are governed by the Klein-Gordon (KG) equation [29, 30]

$$\ddot{\phi} + 3H\dot{\phi} + \frac{dV(\phi)}{d\phi} = 0, \quad (5)$$

where a dot means derivation with respect to cosmic time, $H = \dot{a}/a$ is the Hubble rate, and a is the scale factor of the universe. After inflation, the friction term is subdominant and thus we can neglect it. Later, we will revisit the issue of considering the Hubble expansion. Using perturbation theory [31] we can expand the field into powers of a small parameter ϵ as

$$\phi = \epsilon\phi_1 + \epsilon^2\phi_2 + \epsilon^3\phi_3 + \dots \quad (6)$$

If we now substitute this expansion into (5), use (4) and solve order by order we find that at order ϵ^3 the solution behaves in a secular way since one of the driving terms in the differential equation has exactly the fundamental frequency of the system, i.e., M . To avoid this behavior we can use the Lindstedt-Poincaré renormalization procedure, where we expand both the field and the frequency, see [31] for further details. This expansion of the frequency is made by considering the new time variable [7, 8]

$$\tau = t\sqrt{1 - \epsilon^2}. \quad (7)$$

Substitution into (5) of equations (4), (6) and changing to time variable τ gives the following expressions for the expansions of the field

$$\phi_1 = \Phi_1 \cos(M\tau), \quad (8a)$$

$$\phi_2 = \Phi_2(\cos(2M\tau) - 3), \quad (8b)$$

where

$$\Phi_1 = \frac{2M}{\sqrt{3\left|\lambda - \frac{10\lambda_3^2}{9M^2}\right|}}, \quad \Phi_2 = \frac{\lambda_3}{6M^2}\Phi_1^2. \quad (9)$$

The amplitude Φ_1 is fixed when eliminating the secular term in the differential equation for ϕ_3 . The solution to this last is not shown since we will work up to order ϵ^2 . Regarding the asymmetric (with respect to the origin) term ϕ_2 of the expansion, we see that it is proportional to λ_3 . Thus we clearly see that the asymmetry of the potential is transferred to the solution of the field. For symmetric potentials ($\lambda_3 = 0 \neq \lambda$), the solution to $\mathcal{O}(\epsilon^2)$ is given by $\phi = \epsilon\phi_1 + \mathcal{O}(\epsilon^3)$, which is closer to the quadratic potential.

At this point, it is interesting to introduce the decay of the field. We have solved (5) without considering the Hubble friction term, which makes the field's amplitude constant in time. To include it, it is enough to parameterize ϵ as

$$\epsilon(\tau) = \epsilon_{\text{end}} \left(\frac{a_{\text{end}}}{a}\right)^{3/2}, \quad (10)$$

where a_{end} is the scale factor evaluated at the end of inflation, τ_{end} , and ϵ_{end} is obtained from (6) evaluated at $\tau = \tau_{\text{end}}$ up to the desired order. To simplify notation we omit the argument of ϵ . Also, we neglect derivatives of ϵ , since it is assumed to vary slowly.

3.2 Floquet theory for perturbations

The evolution of the scalar perturbations is controlled by the so-called MS variable $v_{\mathbf{k}}$ [9, 29, 30]. The MS equation expressed in the time variable τ is written as

$$\tilde{v}_{\mathbf{k}}'' + \left(\frac{k^2}{a^2} + \frac{d^2V}{d\phi^2} + 3\phi'^2 - \frac{\phi'^4}{2H^2} + \frac{3}{4}\left(\frac{\phi'^2}{2} - V\right) + \frac{2\phi'}{H}\frac{dV}{d\phi}\right)(1 + \epsilon^2)\tilde{v}_{\mathbf{k}} = 0, \quad (11)$$

where a tilde means derivation with respect to τ , $\tilde{v}_{\mathbf{k}} = a^{1/2}v_{\mathbf{k}}$ is the re-scaled MS variable [10, 11, 32] and we have expanded $(1 - \epsilon^2)^{-1} \simeq 1 + \epsilon^2 + \mathcal{O}(\epsilon^4)$, which comes from changing from t to τ in $\tilde{v}_{\mathbf{k}}''$. Substituting in (11) the expansion of the potential (4) together with the expansion of the field (6) and making $z = M\tau = Mt\sqrt{1 - \epsilon^2}$ we find, up to order ϵ^2

$$\frac{d^2\tilde{v}_{\mathbf{k}}}{dz^2} + (A_{\mathbf{k}} + 2q_1 \cos(z) + 2p_1 \sin(z) + 2q_2 \cos(2z) + 2p_2 \sin(2z) + h.h.)\tilde{v}_{\mathbf{k}} = 0, \quad (12)$$

with

$$A_{\mathbf{k}} = \frac{k^2}{a^2 M^2} + 1 + \left(1 + \left(\frac{3}{2} + \frac{3\lambda}{2M^2} - \frac{\lambda_3^2}{M^4}\right)\Phi_1^2\right)\epsilon^2, \quad (13a)$$

$$q_1 = \frac{\lambda_3 \Phi_1 \epsilon}{M^2}, \quad (13b)$$

$$p_1 = - \left(\sqrt{\frac{3}{2}} - \sqrt{\frac{25}{6}} \right) \frac{\lambda_3 \Phi_1^2 \epsilon^2}{2M^2}, \quad (13c)$$

$$q_2 = \left(\frac{3\lambda}{2M^2} + \frac{\lambda_3^2}{3M^4} - \frac{3}{2} \right) \frac{\Phi_1^2 \epsilon^2}{2}, \quad (13d)$$

$$p_2 = -\sqrt{\frac{3}{2}} \Phi_1 \epsilon, \quad (13e)$$

and where *h.h.* in (12) stands for higher harmonics. We do not consider them since doing so would introduce a higher order in ϵ when calculating the Floquet exponent [33]. To derive (12) we have used also that the Hubble rate is given up to $\mathcal{O}(\epsilon^2)$ by

$$H^2 = \frac{1}{3} \left(\frac{\dot{\phi}^2}{2} + V \right) = \frac{\epsilon^2 M^2 \Phi_1^2}{6}. \quad (14)$$

Eqn. (12) is known as a Hill equation, a generalization of a Mathieu equation [6–9]. Depending on the values of the parameters A_k , q_i , and p_i the physical modes $(\frac{k}{a})^{-1}$ experience instability or stability as they evolve. Following Floquet's theorem, the re-scaled MS variable evolves as $\tilde{v}_{\mathbf{k}} \sim e^{\int \mu_{\mathbf{k}}(z) dz}$, where $\mu_{\mathbf{k}}$ are the so-called *Floquet exponents*. For $\Re(\mu_{\mathbf{k}}) > 0$ we have exponential growth and the mode is said to be unstable. The Floquet exponents of the Hill equation are generally unknown but can be computed using the harmonic balance method. In this work, we will apply the method outlined in [7, 8] (see also Appendix A of [34]). In order to solve (11), the MS variable $\tilde{v}_{\mathbf{k}}$ is expanded into harmonics as

$$\tilde{v}_{\mathbf{k}} = \sum_{n=0}^{\infty} e^{inz} C_n(z). \quad (15)$$

By substituting this into (12) and expressing the trigonometric functions as complex exponential functions, the following recurrence relation is obtained

$$\begin{aligned} \frac{dC_n}{dz} = \frac{i}{2n} [(A_k - n^2)C_n + q_1(C_{n+1} + C_{n-1}) + ip_1(C_{n+1} - C_{n-1}) + \\ + q_2(C_{n+2} + C_{n-2}) + ip_2(C_{n+2} - C_{n-2})], \end{aligned} \quad (16)$$

where we are neglecting $\frac{d^2 C_n}{dz^2}$ since we assume that C_n are slowly varying. The first instability band emerges from examining the fundamental frequencies $n = \pm 1$ in (16). Typically, to order ϵ^2 , the coefficients $C_{\pm 1}$ are coupled just one to each other. However, in our case, the presence of q_1 and p_1 , along with q_1 and p_2 being of order ϵ , the coefficients $C_{\pm 1}$ are also being coupled to C_0 , $C_{\pm 2}$ and $C_{\pm 3}$ to order ϵ^2 . This additional coupling complicates the computation of the Floquet exponents. Nonetheless, we have found that it suffices for our purposes to consider the fundamental frequencies $n = \pm 1$ and their corresponding couplings with the nearest harmonics $n = 0, 2$ and $n = -2, 0$, respectively, up to order ϵ^2 . By doing this, we derive the following differential matrix

equation

$$\frac{d}{dz} \begin{pmatrix} C_1 \\ C_{-1} \end{pmatrix} \simeq \frac{i}{2} \begin{pmatrix} A_k - 1 - \frac{q_1^2 + p_1^2}{A_k} - \frac{q_1^2 + p_1^2}{A_k - 4} & q_2 - ip_2 - \frac{(q_1 - ip_1)^2}{A_k} \\ -q_2 - ip_2 - \frac{(q_1 + ip_1)^2}{A_k} & 1 - A_k + \frac{q_1^2 + p_1^2}{A_k} + \frac{q_1^2 + p_1^2}{A_k - 4} \end{pmatrix} \begin{pmatrix} C_1 \\ C_{-1} \end{pmatrix}. \quad (17)$$

Finally, remembering Floquet's theorem, the re-scaled MS variable evolves as $\tilde{v}_{\mathbf{k}} \simeq e^{\int \mu_{\mathbf{k}}(z) dz}$ [9], where $\mu_{\mathbf{k}}(z)$ are now given by the eigenvalues of the matrix in (17). Up to order ϵ^2 , these are given by²:

$$\mu_{\mathbf{k}} = \pm \frac{1}{2} \left[q_2^2 + p_2^2 - (A_k - 1)^2 + 2q_1^2 \left(\frac{A_k - 1}{A_k} + \frac{A_k - 1}{A_k - 4} - \frac{q_1^2}{2(A_k - 4)^2} - \frac{q_1^2}{A_k(A_k - 4)} \right) + 2p_1^2 \left(\frac{A_k - 1}{A_k} + \frac{A_k - 1}{A_k - 4} \right) - \frac{2q_1^2 q_2}{A_k} - \frac{4p_1 p_2 q_1}{A_k} \right]^{1/2}. \quad (18)$$

We can relate the MS variable to the comoving curvature perturbation $\mathcal{R}_{\mathbf{k}}$ by

$$\mathcal{R}_{\mathbf{k}} = \frac{v_{\mathbf{k}}}{\sqrt{2\epsilon_H a}} = \frac{\tilde{v}_{\mathbf{k}}}{\sqrt{2\epsilon_H a^3}}, \quad (19)$$

where $\epsilon_H = -\dot{H}/H^2$ is the Hubble slow-roll parameter. From (19) we see that when the amplification of $\tilde{v}_{\mathbf{k}}$ exceeds $a^{3/2}$, the curvature perturbation will grow. Typically, for potentials close to parabolic, this amplification is as high as $a^{3/2}$, causing $\mathcal{R}_{\mathbf{k}}$ to remain approximately constant for the modes inside the resonance band [10]. However, as we demonstrate in the next section, deviating from quadratic behavior alters the scenario, producing a fast amplification in a specific range of modes.

4 Characterization of self-resonance

Here we present the Floquet's exponents for both T- and E-models and compare them with numerical results. These findings can be generalized to any potential whose expansion around $\phi = 0$ matches either the expansion of a T- or an E-model.

4.1 T-model

In this case we have that $\lambda_3 = 0$ and thus $q_1 = p_1 = 0$, which greatly simplifies the expression for the Floquet exponent

$$\mu_{\mathbf{k}}^{(T)} = \frac{1}{2} \sqrt{q_2^2 + p_2^2 - (A_k - 1)^2}. \quad (20)$$

For the rest of this work, we set $\alpha = 10^{-2.5}$ for both T- and E-models. To check the validity of this approximation, we have computed the curvature perturbations numerically, using (11) with Bunch-Davies initial conditions and (19). Then, we have used the Floquet theory derived here. Both methods are evaluated 5 e-folds after the end

²Since we are interested only in amplification we will consider just the one with the + sign.

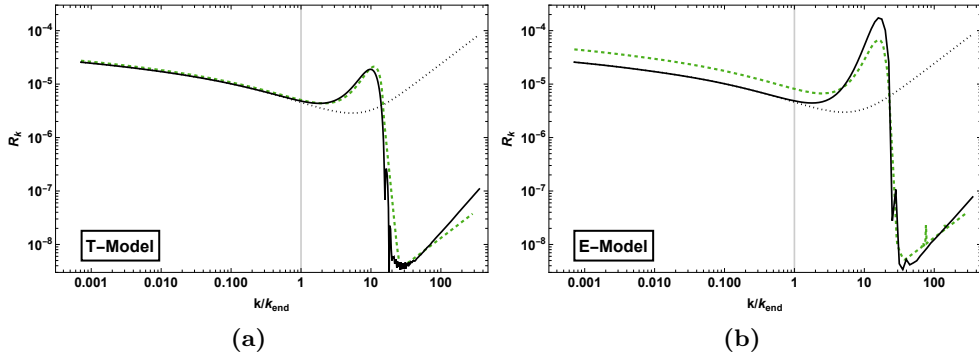


Fig. 1: Curvature perturbations for (a) T-model and (b) E-model evaluated 5 e-folds after the end of inflation. Numerical computation is shown in continuous black and Floquet theory as described in this work in dashed green. The vertical grey line marks the scale that exits the horizon at the end of inflation, k_{end} . For comparison, black dotted curves show the numerical computation of curvature perturbations at the end of inflation.

of inflation. Results are displayed in Fig. 1a and it shows a good agreement between both methods. The peaks to the right of the highest peak in Fig. 1 correspond to the amplification in higher resonance bands. One could study these bands by considering the frequencies $n = \pm 2, \pm 3 \dots$ and their corresponding couplings. However, to do so, one has to increase each time the order in ϵ , increasing the number of harmonics that come into play. We find it sufficient for our purposes to focus on the first resonance band, as it is where the amplification is most pronounced. Finally, in Fig. 2a we display $\Re(\mu_k^{(T)})$ as a function of q_2 and A_k , as well as the trajectories of some modes in the (q_2, A_k) plane. We remark that in Fig. 2a, $p_2 = 0$ and thus the $\mu_k^{(T)}$ shown does not correspond to the real time-evolution. However, it is enough to understand why the peak is produced for scales around $k \simeq 10 k_{\text{end}}$. Those scales cross the (q_2, A_k) plane throughout the maximum of $\mu_k^{(T)}$. For $k < k_{\text{end}}$, all scales show the same evolution in the (q_2, A_k) plane. This is the reason why all of them are amplified in the same amount.

4.2 E-model

Now we have that $\lambda_3 \neq 0$ and thus the expression for the Floquet exponent is the full one given in (18), we will call it $\mu_k^{(E)}$. Fig. 1b displays the curvature perturbations computed using the same method as in Fig. 1a (see previous section), this time for the E-model. Despite a numerical factor of $\mathcal{O}(1)$ of discrepancy between the numerics and Floquet theory, we find it enough to explain at which scales occur the maximum amplification. The discrepancy could be because we are neglecting some higher harmonics, which in the case of the E-model could contribute more significantly than in the T-model, as well as more couplings between them. A comparison between Figs. 1a and 1b reveals a higher amplification for the E-model compared to the T-model, for the same value of α . Additionally, the position of the peak of maximum amplification is at higher k for the E-model. Now, regarding the time evolution of $\mu_k^{(E)}$ for

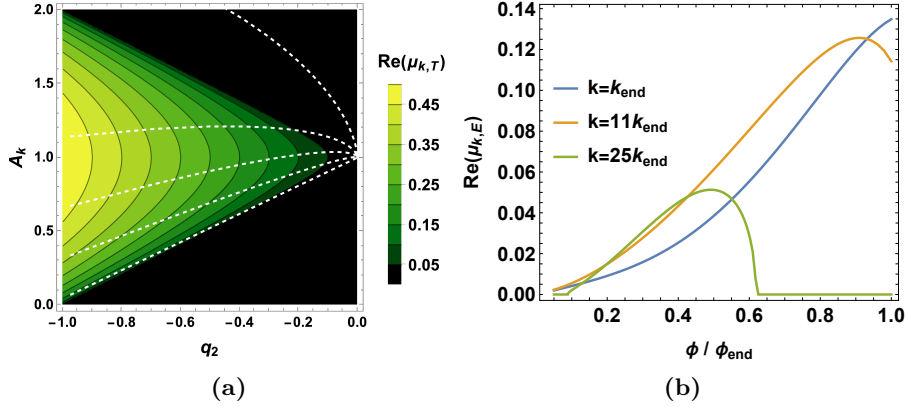


Fig. 2: (a) Floquet chart for a T-model with $p_2 = 0$ (just for graphical purposes). White dashed lines correspond to the evolution of the modes in the (q_2, A_k) plane and are, from bottom to top: 1, 10, 15, 20, 30, in units of k_{end} . (b) Evolution of $\Re(\mu_{k,E})$ for an E-model as a function of the amplitude of the field and for different values of k .

each k -mode, a plot like Fig. 2a would not be sufficiently illustrative, given that $\mu_k^{(E)}$ depends on 5 parameters. This makes it challenging to understand why the peak is around $k \sim 11 k_{\text{end}}$. Instead, Fig. 2b shows $\Re(\mu_k^{(E)})$ as a function of the amplitude of the field for different values of k , expressed in units of k_{end} . Here, we observe that for scales around $k \simeq 11 k_{\text{end}}$, the Floquet exponent exceeds that of other k -modes, resulting in higher amplification.

5 Contrast with quadratic approximation

During preheating, the potential is usually approximated by a parabola ($\lambda_3 = \lambda = 0$), where the solution for the field is just given by $\phi \simeq \phi_{\text{end}} \left(\frac{a_{\text{end}}}{a}\right)^{3/2} \cos(Mt)$ [9]. Considering this and keeping just the dominant terms, (11) is easily reformulated into the following Mathieu equation

$$\frac{d^2 \tilde{v}_k}{dz^2} + (A_k + 2p_2 \sin(2z)) \tilde{v}_k = 0, \quad (21)$$

where now $z = Mt$ and

$$A_k = \frac{k^2}{a^2 M^2} + 1, \quad p_2 = -\sqrt{\frac{3}{2}} \phi_{\text{end}} \left(\frac{a_{\text{end}}}{a}\right)^{3/2}. \quad (22)$$

Following the steps of Sec. 3.2, the Floquet exponent is given by

$$\mu_k^{(Q)} = \frac{1}{2} \sqrt{p_2^2 - (A_k - 1)^2}. \quad (23)$$

Let us now introduce the concept of *instability scale*, denoted as l_{inst} , which represents the spatial scale above which \tilde{v}_k experiences growth. For this growth to occur, the

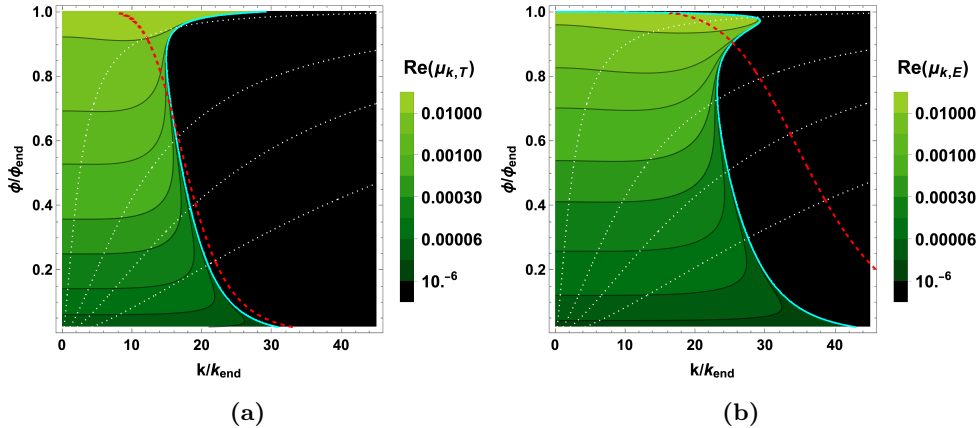


Fig. 3: Floquet exponents for (a) T-model and (b) E-model as a function of physical wavenumbers and field amplitudes. Red dashed lines represent the instability scale (24) and continuous cyan lines the corresponding instability scales for the full expansion (4). For the T-model, this last is given by (25), whereas for the E-model is obtained numerically. White dotted lines mark the evolution of the physical k -modes. The black region represents the points where $\Re(\mu_k^{(T,E)}) = 0$.

Floquet exponent must be real and positive. Imposing this in (23) and solving for $(\frac{k}{a})^{-1} \sim l_{\text{inst}}$, one obtains

$$l_{\text{inst}}^{(Q)} = \frac{1}{M} \left(\frac{2}{3\phi_{\text{end}}^2} \left(\frac{a}{a_{\text{end}}} \right)^3 \right)^{1/4} \simeq \frac{1}{\sqrt{3HM}}. \quad (24)$$

However, this approximation is not accurate for some potentials, even if they behave as quadratic at first order, such as the case of α -attractors with $\alpha \ll 1$. Fig. 3 corroborates this fact. It shows the Floquet exponent for both the T- and E-models and compares, in each case, $l_{\text{inst}}^{(Q)}$ (dashed red) with the corresponding spatial scale $l_{\text{inst}}^{(T,E)}$ (cyan) of the full expansion (4). For the T-model, imposing again that $\Re(\mu_k^{(T)}) > 0$ in (20) we obtain

$$l_{\text{inst}}^{(T)} = \left(\frac{1}{2} \sqrt{- (4M^2 + 6M^2\Phi_1^2 + 6\lambda\Phi_1^2)\epsilon^2 + \sqrt{24M^4\Phi_1^2\epsilon^2 + 9(M^2 - \lambda)^2\Phi_1^4\epsilon^4}} \right)^{-1}. \quad (25)$$

Looking at the expression for $\mu_k^{(E)}$, eqn. (18), one can observe the difficulty in obtaining an analytical expression for the instability scale in this case. For that reason, in Fig. 3b, $l_{\text{inst}}^{(E)}$ is obtained numerically. White dotted lines represent the evolution of the physical modes, and at the moment those modes cross the instability scale, they start to amplify. These crossing points are different if one uses the full expansion (4) or just the quadratic term, pointing out the importance of considering higher-order terms. Moreover, the enhancement of perturbations can be physically explained with the negativity of the coefficients of the expansion, λ_3 or λ_T . If we treat them as

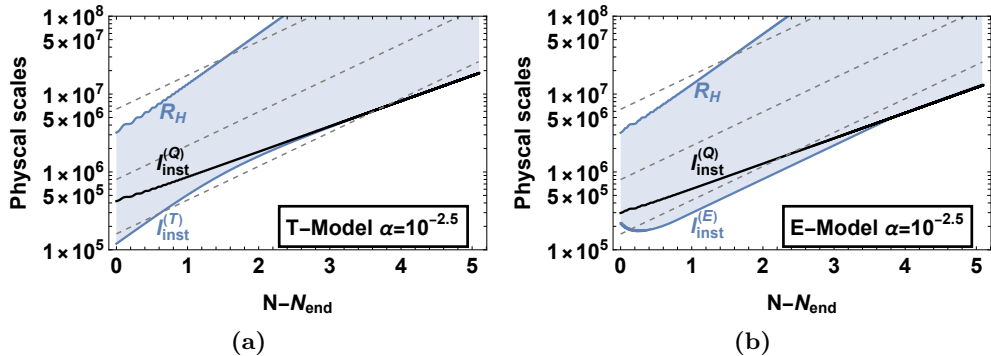


Fig. 4: Instability band (blue shaded area) and instability scales, l_{inst} , for the quadratic case and for a (a) T-model and (b) E-model. Also plotted are the Hubble radius R_H and the evolution of some physical modes $(\frac{k}{a})^{-1}$ (gray dashed lines). The horizontal axis represents the number of e-folds elapsed from the end of inflation.

self-interactions of the field, a negative coefficient implies an attractive force, which induces a negative pressure and makes some modes unstable [7, 8]. Nonetheless, as the field decays, the cubic and quartic terms of the expansion (4) became less dominant and one recovers the usual preheating scenario [6, 10, 11, 35] where the potential is well approximated by a parabola and $\tilde{v}_{\mathbf{k}} \sim a^{3/2}$. This can be seen in Fig. 3a, where for small amplitudes of the field $l_{\text{inst}}^{(Q)} \sim l_{\text{inst}}^{(T)}$. For Fig. 3b, one should go to smaller amplitudes to have this parallelism. Lastly, it is important to note that not all perturbations with $(\frac{k}{a})^{-1} > l_{\text{inst}}$ undergo amplification. The upper limit is set by the Hubble radius $R_H = H^{-1}$ and the set of modes defined by $R_H > (\frac{k}{a})^{-1} > l_{\text{inst}}$ is usually called *instability band* (IB). Figs. 4a and 4b show the IB (blue shaded area) for a T- and an E-model, respectively. We see again that, for the T-model, $l_{\text{inst}}^{(T)}$ approaches $l_{\text{inst}}^{(Q)}$ sooner than in the E-model case. This is mainly because the former one is closer to the parabola, given the absence of the asymmetric coefficient λ_3 . If we neglect the higher-order terms in the expansion of the potential then we are not considering the amplification of some modes that enter the IB around the beginning of preheating, indicated by the lower gray dashed lines.

6 Applications

Floquet theory offers a significant advantage: it allows us to forget about numerical computations and use the analytical results to estimate how the curvature perturbations are amplified. This approach accelerates computations, which typically imply long computational times associated with the highly oscillatory regime of preheating. Furthermore, the amplification process can lead to intriguing phenomena, as we briefly outline in the following discussion.

- **Primordial Black Holes:** Using general relativity one can study the collapse into a black hole (BH) of a real, minimally coupled, massive scalar field in an asymptotically Einstein-de Sitter spacetime background. In [10, 36, 37] it is shown

that density perturbations $\delta\rho_{\mathbf{k}}$ can collapse into a BH provided that the time the k -mode spends inside the IB exceeds the time it needs to collapse, defined as

$$\Delta t_{\text{coll}} = \frac{\pi}{H[t_{\text{bc}}(k)]\delta_{\mathbf{k}}^{3/2}[t_{\text{bc}}(k)]}, \quad (26)$$

where $t_{\text{bc}}(k)$ is the time at which each mode enters the instability band and $\delta_{\mathbf{k}} = \frac{\delta\rho_{\mathbf{k}}}{\rho}$ is the density contrast, being ρ the background energy density and $\delta\rho_{\mathbf{k}}$ the density perturbations. In our specific scenario, perturbations amplify faster with decreasing α values. This suggests that PBHs form more rapidly and consequently with smaller masses. However, a critical threshold should exist where PBHs may become overproduced, thereby establishing a lower bound for α . This is something we intend to study and publish soon somewhere [26]

- **Scalar-Induced Gravitational Waves:** At second order in perturbation theory, the scalar perturbations couple to the tensor ones, inducing the production of GWs [16–20]. The resulting differential equation for the tensor perturbations $h_{\mathbf{k}}(\eta)$ in cosmic time η is given by

$$h_{\mathbf{k}}''(\eta) + 2\mathcal{H}h_{\mathbf{k}}'(\eta) + k^2h_{\mathbf{k}}(\eta) = \mathcal{S}(\mathbf{k}, \eta), \quad (27)$$

where $\mathcal{H} = aH$ is the conformal Hubble rate and $\mathcal{S}(\mathbf{k}, \eta)$ is the so-called source function, which directly depends on the metric scalar perturbation $\Phi_{\mathbf{k}}$. This last can be related to the curvature perturbation $\mathcal{R}_{\mathbf{k}}$ [35] and thus with $v_{\mathbf{k}}$, which again suggests that for decreasing values of α the fractional energy density of GWs, $\Omega_{\text{GW}}(k)$, can be high enough to reach the range of detection of some actual and future GWs detectors [38, 39]. The fractional energy density is defined as [18]

$$\Omega_{\text{GW}}(k) \equiv \frac{1}{\rho} \frac{d\rho_{\text{GW}}}{d \ln k} = \frac{k^2}{12\mathcal{H}^2} \sum_{\theta} \mathcal{P}_{h,\theta}(k), \quad (28)$$

where ρ_{GW} is the energy density of GWs and $\mathcal{P}_{h,\theta}(k)$ the power spectrum of tensor perturbations, with θ accounting for both polarization states. We will also study this and publish our findings [27]

- **Oscillons:** Oscillons are defined as relatively long-lived and spatially localized regions where a scalar field oscillates with large amplitude [21–25]. They form when the inflationary potential deviates from parabolic shape and could leave some imprint in the present-day universe, particularly in the form of GWs.

7 Conclusions

This work introduces an analytical model to explain the amplification of curvature perturbations at small scales during the post-inflationary preheating phase, based on the phenomenon of self-resonance. Initially, we solve perturbatively for the inflaton field and expand the inflationary potential up to fourth order. Then, we transform the MS (11) equation into a Hill’s one (12) and provide an explicit formula (18) for

Floquet's exponents of the MS variable. This, so far in the literature, was not given when the potential includes both cubic and quartic self-interactions. Traditionally, self-resonance has been studied primarily within the framework of the perturbed Klein-Gordon equation. However, our approach is applied to the MS equation, since it is more complete in the sense of describing perturbations. While applicable to any potential that can be expressed as (4), we focus our analysis on α -attractor models, given their observational favorability [5]. Particularly, for $\alpha \ll 1$, our model reveals a pronounced self-resonance effect, leading to a rapid and substantial enhancement of the curvature perturbations. This analytical model is compared with a full numerical computation, as can be seen in Fig. 1, showing a good agreement, especially concerning the T-model. Also, we stress the importance of avoiding the parabola approximation during preheating for some models, specifically during the transition from inflation to preheating, as illustrated in Figs. 3 and 4. Moreover, this investigation opens a window on the potential role of α -attractors in the formation of PBHs on small scales as well as in the production of SIGWs and oscillons during preheating. Furthermore, it suggests a possible physical lower bound on the parameter α , since as we decrease its value, perturbations amplify more drastically, and thus for a very extremely low value of α this could potentially leave an imprint in CMB observations. Finally, we stress that this mechanism of amplification of perturbations is inherent to preheating in α -attractor models and does not require any fine-tuning.

Acknowledgements. I express my gratitude to João Marto and K. Sravan Kumar for their valuable suggestions and assistance in the development of this work. I am also grateful for the support of grant UI/BD/151491/2021 from the Portuguese Agency Fundação para a Ciência e a Tecnologia. This research was funded by Fundação para a Ciência e a Tecnologia grant number UIDB/MAT/00212/2020.

References

- [1] Kallosh, R., Linde, A.: Multi-field Conformal Cosmological Attractors. JCAP **12**, 006 (2013) <https://doi.org/10.1088/1475-7516/2013/12/006> arXiv:1309.2015 [hep-th]
- [2] Kallosh, R., Linde, A.: Universality Class in Conformal Inflation. JCAP **07**, 002 (2013) <https://doi.org/10.1088/1475-7516/2013/07/002> arXiv:1306.5220 [hep-th]
- [3] Kaiser, D.I., Sfakianakis, E.I.: Multifield Inflation after Planck: The Case for Nonminimal Couplings. Phys. Rev. Lett. **112**(1), 011302 (2014) <https://doi.org/10.1103/PhysRevLett.112.011302> arXiv:1304.0363 [astro-ph.CO]
- [4] Kallosh, R., Linde, A.: Planck, LHC, and α -attractors. Phys. Rev. D **91**, 083528 (2015) <https://doi.org/10.1103/PhysRevD.91.083528> arXiv:1502.07733 [astro-ph.CO]
- [5] Akrami, Y., *et al.*: Planck 2018 results. X. Constraints on inflation. Astron. Astrophys. **641**, 10 (2020) <https://doi.org/10.1051/0004-6361/201833887>

arXiv:1807.06211 [astro-ph.CO]

- [6] Kofman, L., Linde, A.D., Starobinsky, A.A.: Towards the theory of reheating after inflation. *Phys. Rev. D* **56**, 3258–3295 (1997) <https://doi.org/10.1103/PhysRevD.56.3258> arXiv:hep-ph/9704452
- [7] Hertzberg, M.P., Karouby, J., Spitzer, W.G., Becerra, J.C., Li, L.: Theory of self-resonance after inflation. I. Adiabatic and isocurvature Goldstone modes. *Phys. Rev. D* **90**, 123528 (2014) <https://doi.org/10.1103/PhysRevD.90.123528> arXiv:1408.1396 [hep-th]
- [8] Hertzberg, M.P., Karouby, J., Spitzer, W.G., Becerra, J.C., Li, L.: Theory of self-resonance after inflation. II. Quantum mechanics and particle-antiparticle asymmetry. *Phys. Rev. D* **90**, 123529 (2014) <https://doi.org/10.1103/PhysRevD.90.123529> arXiv:1408.1398 [hep-th]
- [9] Jedamzik, K., Lemoine, M., Martin, J.: Collapse of Small-Scale Density Perturbations during Preheating in Single Field Inflation. *JCAP* **09**, 034 (2010) <https://doi.org/10.1088/1475-7516/2010/09/034> arXiv:1002.3039 [astro-ph.CO]
- [10] Martin, J., Papanikolaou, T., Vennin, V.: Primordial black holes from the preheating instability in single-field inflation. *JCAP* **01**, 024 (2020) <https://doi.org/10.1088/1475-7516/2020/01/024> arXiv:1907.04236 [astro-ph.CO]
- [11] Martin, J., Papanikolaou, T., Pinol, L., Vennin, V.: Metric preheating and radiative decay in single-field inflation. *JCAP* **05**, 003 (2020) <https://doi.org/10.1088/1475-7516/2020/05/003> arXiv:2002.01820 [astro-ph.CO]
- [12] Zel'dovich, Y.B., Novikov, I.D.: The Hypothesis of Cores Retarded during Expansion and the Hot Cosmological Model. *Soviet Astron. AJ (Engl. Transl.)*, **10**, 602 (1967)
- [13] Hawking, S.: Gravitationally collapsed objects of very low mass. *Mon. Not. Roy. Astron. Soc.* **152**, 75 (1971) <https://doi.org/10.1093/mnras/152.1.75>
- [14] Carr, B.J., Hawking, S.W.: Black holes in the early Universe. *Mon. Not. Roy. Astron. Soc.* **168**, 399–415 (1974) <https://doi.org/10.1093/mnras/168.2.399>
- [15] Carr, B.J.: The Primordial black hole mass spectrum. *Astrophys. J.* **201**, 1–19 (1975) <https://doi.org/10.1086/153853>
- [16] Maggiore, M.: *Gravitational Waves. Vol. 1: Theory and Experiments.* Oxford University Press, ??? (2007). <https://doi.org/10.1093/acprof:oso/9780198570745.001.0001>
- [17] Guzzetti, M.C., Bartolo, N., Liguori, M., Matarrese, S.: Gravitational waves from inflation. *Riv. Nuovo Cim.* **39**(9), 399–495 (2016) <https://doi.org/10.1393/ncr/>

[i2016-10127-1](#) [arXiv:1605.01615](#) [astro-ph.CO]

- [18] Domènech, G.: Scalar Induced Gravitational Waves Review. *Universe* **7**(11), 398 (2021) <https://doi.org/10.3390/universe7110398> [arXiv:2109.01398](#) [gr-qc]
- [19] Baumann, D., Steinhardt, P.J., Takahashi, K., Ichiki, K.: Gravitational Wave Spectrum Induced by Primordial Scalar Perturbations. *Phys. Rev. D* **76**, 084019 (2007) <https://doi.org/10.1103/PhysRevD.76.084019> [arXiv:hep-th/0703290](#)
- [20] Ananda, K.N., Clarkson, C., Wands, D.: The Cosmological gravitational wave background from primordial density perturbations. *Phys. Rev. D* **75**, 123518 (2007) <https://doi.org/10.1103/PhysRevD.75.123518> [arXiv:gr-qc/0612013](#)
- [21] Amin, M.A., Easther, R., Finkel, H.: Inflaton Fragmentation and Oscillon Formation in Three Dimensions. *JCAP* **12**, 001 (2010) <https://doi.org/10.1088/1475-7516/2010/12/001> [arXiv:1009.2505](#) [astro-ph.CO]
- [22] Amin, M.A., Easther, R., Finkel, H., Flauger, R., Hertzberg, M.P.: Oscillons After Inflation. *Phys. Rev. Lett.* **108**, 241302 (2012) <https://doi.org/10.1103/PhysRevLett.108.241302> [arXiv:1106.3335](#) [astro-ph.CO]
- [23] Gleiser, M., Graham, N., Stamatopoulos, N.: Generation of Coherent Structures After Cosmic Inflation. *Phys. Rev. D* **83**, 096010 (2011) <https://doi.org/10.1103/PhysRevD.83.096010> [arXiv:1103.1911](#) [hep-th]
- [24] Antusch, S., Cefala, F., Orani, S.: Gravitational waves from oscillons after inflation. *Phys. Rev. Lett.* **118**(1), 011303 (2017) <https://doi.org/10.1103/PhysRevLett.118.011303> [arXiv:1607.01314](#) [astro-ph.CO]. [Erratum: *Phys.Rev.Lett.* 120, 219901 (2018)]
- [25] Zhou, S.-Y., Copeland, E.J., Easther, R., Finkel, H., Mou, Z.-G., Saffin, P.M.: Gravitational Waves from Oscillon Preheating. *JHEP* **10**, 026 (2013) [https://doi.org/10.1007/JHEP10\(2013\)026](https://doi.org/10.1007/JHEP10(2013)026) [arXiv:1304.6094](#) [astro-ph.CO]
- [26] del-Corral, D., Gondolo, P., Kumar, K.S., Marto, J.: Primordial black holes through preheating instabilities in α -attractor models [arXiv:2407.XXXX](#) [astro-ph.CO]
- [27] del-Corral, D., Gondolo, P., Kumar, K.S., Marto, J.: Scalar-Induced Gravitational Waves during preheating in α -attractor models [arXiv:2407.XXXX](#) [astro-ph.CO]
- [28] Iacconi, L., Fasiello, M., Väiviita, J., Wands, D.: Novel CMB constraints on the α parameter in alpha-attractor models. *JCAP* **10**, 015 (2023) <https://doi.org/10.1088/1475-7516/2023/10/015> [arXiv:2306.00918](#) [astro-ph.CO]
- [29] Baumann, D.: Inflation. In: *Theoretical Advanced Study Institute in Elementary Particle Physics: Physics of the Large and the Small*, pp. 523–686 (2011). https://doi.org/10.1007/978-1-4020-9856-9_15

[//doi.org/10.1142/9789814327183_0010](https://doi.org/10.1142/9789814327183_0010)

- [30] Mukhanov, V.F., Feldman, H.A., Brandenberger, R.H.: Theory of cosmological perturbations. Part 1. Classical perturbations. Part 2. Quantum theory of perturbations. Part 3. Extensions. Phys. Rept. **215**, 203–333 (1992) [https://doi.org/10.1016/0370-1573\(92\)90044-Z](https://doi.org/10.1016/0370-1573(92)90044-Z)
- [31] Drazin, P.G.: Nonlinear Systems. Cambridge Texts in Applied Mathematics. Cambridge University Press, ??? (1992). <https://doi.org/10.1017/CBO9781139172455>
- [32] Finelli, F., Brandenberger, R.H.: Parametric amplification of gravitational fluctuations during reheating. Phys. Rev. Lett. **82**, 1362–1365 (1999) <https://doi.org/10.1103/PhysRevLett.82.1362> [arXiv:hep-ph/9809490](https://arxiv.org/abs/hep-ph/9809490)
- [33] Amin, M.A.: Inflaton fragmentation: Emergence of pseudo-stable inflaton lumps (oscillons) after inflation (2010) [arXiv:1006.3075](https://arxiv.org/abs/1006.3075) [astro-ph.CO]
- [34] Enqvist, K., Karčiauskas, M., Lebedev, O., Rusak, S., Zatta, M.: Postinflationary vacuum instability and Higgs-inflaton couplings. JCAP **11**, 025 (2016) <https://doi.org/10.1088/1475-7516/2016/11/025> [arXiv:1608.08848](https://arxiv.org/abs/1608.08848) [hep-ph]
- [35] del-Corral, D., Gondolo, P., Kumar, K.S., Marto, J.: Revisiting primordial black holes formation from preheating instabilities: the case of Starobinsky inflation (2023) [arXiv:2311.02754](https://arxiv.org/abs/2311.02754) [astro-ph.CO]
- [36] Goncalves, S.M.C.V.: Black hole formation from massive scalar field collapse in the Einstein-de Sitter universe. Phys. Rev. D **62**, 124006 (2000) <https://doi.org/10.1103/PhysRevD.62.124006> [arXiv:gr-qc/0008039](https://arxiv.org/abs/gr-qc/0008039)
- [37] Barroso, E.J., Demétrio, L.F., Viteni, S.D.P., Ye, X.: Primordial Black Hole Formation in a Dust Bouncing Model (2024) [arXiv:2405.00207](https://arxiv.org/abs/2405.00207) [astro-ph.CO]
- [38] Gehrman, T.C., Shams Es Haghi, B., Sinha, K., Xu, T.: Baryogenesis, primordial black holes and MHz–GHz gravitational waves. JCAP **02**, 062 (2023) <https://doi.org/10.1088/1475-7516/2023/02/062> [arXiv:2211.08431](https://arxiv.org/abs/2211.08431) [hep-ph]
- [39] Aggarwal, N., *et al.*: Challenges and opportunities of gravitational-wave searches at MHz to GHz frequencies. Living Rev. Rel. **24**(1), 4 (2021) <https://doi.org/10.1007/s41114-021-00032-5> [arXiv:2011.12414](https://arxiv.org/abs/2011.12414) [gr-qc]